Mechanism of Ethylene Oligomerization by a Cationic Palladium(II) Alkyl Complex that Contains a (3,5-Me_2-pyrazolyl)$_2$CHSi(*p*-tolyl)$_3$) Ligand

Matthew P. Conley, Christopher T. Burns, and Richard F. Jordan*

Department of Chemistry, The University of Chicago, 5735 South Ellis Avenue, Chicago, Illinois 60637

Received July 29, 2007

The reactivity of the ethylene oligomerization catalyst (N^N)Pd(Me)(ethylene)$^+$ (**5**), which contains a silyl-capped bis-pyrazolyl methane ligand (N^N = (3,5-Me_2-pyrazolyl)$_2$CHSi(*p*-tolyl)$_3$ (**1**)) was investigated. The reaction of (N^N)PdMeCl (**3**) with Li[B(C_6F_5)$_4$] and ethylene in CH_2Cl_2 generates **5**. Complex **5** undergoes ethylene insertion at −10 °C with a rate constant of $k_{insert,Me} = 3.3(3) \times 10^{-3}$ s^{-1}. Complex **5** catalytically oligomerizes ethylene to branched C_6–C_{20} internal olefins (−10 to 20 °C; 2.7–30 atm ethylene). NMR studies show that an equilibrium mixture of base-free β-agostic secondary alkyl (N^N)PdR$^+$ species (**8**) and ethylene adducts (N^N)Pd(R)(ethylene)$^+$ (**9**) is present under oligomerization conditions. Complex **9** decomposes to Pd^0 at 20 °C, resulting in catalyst decomposition. (N^N)Pd(R)(L)$^+$ species containing R groups that can function as internal donors (either η^2-acyl or agostic β-H) undergo a dynamic process that exchanges the two pz* rings and are thermally unstable. It is proposed that catalyst decomposition and pz* exchange both involve initial coordination of the internal donor to generate a configurationally labile five-coordinate intermediate, which isomerizes, resulting in pz* site exchange or displacement of one arm of the N^N ligand.

Introduction

The ethylene oligomerization and polymerization reactivity of (N^N)PdR(C_2H_4)$^+$ species that contain bis(*N*-heterocycle)-methane (N^N) donor ligands was explored in previous work.[1] (N^N)PdR$^+$ cations that contain sterically small N^N ligands catalytically dimerize ethylene by an insertion/β-H elimination mechanism. The catalyst resting state is the (N^N)Pd(Et)-(ethylene)$^+$ complex. Incorporation of bulky substituents in the bridging methylene position of the N^N ligand shifts the product distribution to higher molecular weight due to inhibition of chain transfer. Increasing the electrophilic character (*N*-heterocycle = imidazole < pyridine < pyrazole) and the steric bulk of the (N^N)Pd unit leads to moderate (up to ca. 10-fold) increases in ethylene insertion rates of (N^N)Pd(R)(ethylene)$^+$ species. During this work, we discovered that the {(*p*-tolyl)$_3$Si)CH-(pz*)$_2$}PdMe$^+$ cation (pz* = 3,5-Me_2-pyrazole), which contains a silyl-capped bis-pyrazolyl-methane ligand, displays unique reactivity. This species exhibits higher ethylene insertion and oligomerization rates but is much less thermally stable compared to other (N^N)PdR$^+$ cations. Here we describe a detailed study of the {(*p*-tolyl)$_3$Si)CH(pz*)$_2$PdMe$^+$ catalyst aimed at understanding the oligomerization behavior and the low thermal stability of this system.

Scheme 1

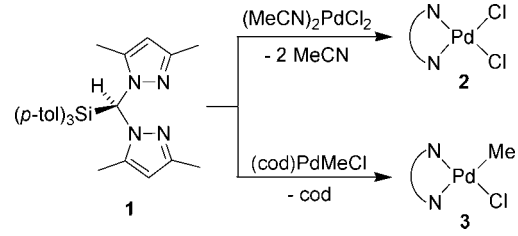

Results and Discussion

Synthesis and Structure of (N^N)PdCl$_2$ and (N^N)PdMeCl. The bis-pyrazolyl methane ligand (*p*-tolyl)$_3$SiCH(pz*)$_2$ (**1**) was prepared by deprotonation of (pz*)$_2$CH$_2$ with ^{n}BuLi in THF at −78 °C, followed by reaction with (*p*-tolyl)$_3$SiOTf. The reaction of **1** with (MeCN)$_2$PdCl$_2$ affords {(*p*-tolyl)$_3$SiCH(pz*)$_2$}PdCl$_2$ (**2**, Scheme 1). The solid state structure of **2** was determined by X-ray diffraction (Figure 1) and is similar to those of other {bis(*N*-heterocycle)methane}Pd^{II} complexes.[1b,c,2] The geometry at Pd is square planar, the (N^N)Pd chelate ring has a boat conformation, and the (*p*-tolyl)$_3$Si group occupies the axial position on the bridging carbon. The ^{1}H NMR spectrum of **2** contains one set of pz* resonances, consistent with C_s symmetry. The spectrum also contains one set of sharp *p*-tolyl resonances, indicating that rotation around the Si−CH and Si−tolyl bonds is fast on the NMR time scale.

The reaction of **1** with (COD)PdMeCl affords {(*p*-tolyl)$_3$SiCH(pz*)$_2$}PdMeCl (**3**, Scheme 1). The ^{1}H NMR spectrum of **3** at 25 °C in CD_2Cl_2 solution contains two sets of

* Corresponding author. E-mail: rfjordan@uchicago.edu.

(1) (a) Burns, C. T.; Jordan, R. F. *Organometallics* **2007**, *26*, 6726. (b) Burns, C. T.; Jordan, R. F. *Organometallics* **2007**, *26*, 6737. (c) Tsuji, S.; Swenson, D. C.; Jordan, R. F. *Organometallics* **1999**, *18*, 4758. For studies of related L$_2$PdR$^+$species see:. (d) Rix, F. C.; Brookhart, M. *J. Am. Chem. Soc.* **1995**, *117*, 1137. (e) Rix, F. C.; Brookhart, M.; White, P. S. *J. Am. Chem. Soc.* **1996**, *118*, 4746. (f) Ittel, S. D.; Johnson, L. K.; Brookhart, M. *Chem. Rev.* **2000**, *100*, 1169. (g) Johnson, L. K.; Killian, C. M.; Brookhart, M. *J. Am. Chem. Soc.* **1995**, *117*, 6414. (h) Mecking, S.; Johnson, L. K.; Wang, L.; Brookhart, M. *J. Am. Chem. Soc.* **1998**, *120*, 888. (i) Temple, D. J.; Johnson, L. K.; Huff, R. L.; White, P. S.; Brookhart, M. *J. Am. Chem. Soc.* **2000**, *122*, 6686. (j) Ikeda, S.; Ohhata, F.; Miyoshi, M.; Tanaka, R.; Minami, T.; Ozawa, F.; Yoshifuji, M. *Angew. Chem., Int. Ed.* **2000**, *39*, 4512. (k) Daugulis, O.; Brookhart, M. *Organometallics* **2002**, *21*, 5926. (l) Doherty, M. D.; Trudeau, S.; White, P. S.; Morken, J. P.; Brookhart, M. *Organometallics* **2007**, *26*, 1261. (m) Ledford, J.; Shultz, C. S.; Gates, D. P.; White, P. S.; DeSimone, J. M.; Brookhart, M. *Organometallics* **2001**, *20*, 5266. (n) Salo, E. V.; Guan, Z. *Organometallics* **2003**, *22*, 5033.

10.1021/om7007698 CCC: $37.00
Publication on Web 12/08/2007

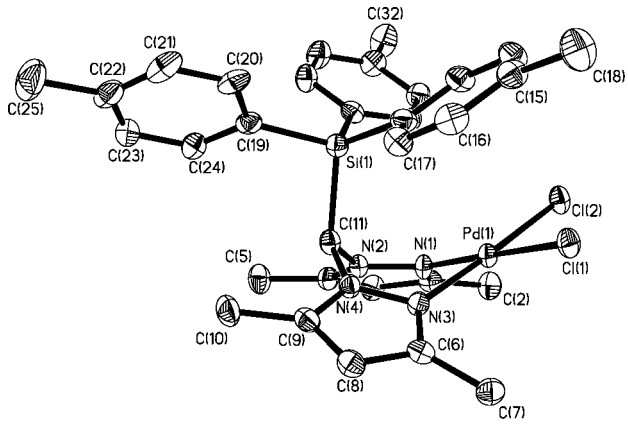

Figure 1. ORTEP view (50% probability ellipsoids) of $\{(p\text{-tolyl})_3SiCH(pz^*)_2\}PdCl_2$ (**2**). H atoms are omitted. Key bond distances (Å) and angles (deg): Pd(1)−Cl(1) 2.28(1); Pd(1)−Cl(2) 2.29(1); N(1)−Pd(1) 2.03(3); N(3)−Pd(1) 2.03(3); N(3)−N(4) 1.38(4); N(1)−N(2) 1.37(4); N(4)−C(11) 1.46(5); N(2)−C(11) 1.45(5); C(11)−Si(1) 1.95(1); N(3)−Pd(1)−N(1) 88.2(1); N(3)−Pd(1)−Cl(1) 91.7(9); N(1)−Pd(1)−Cl(1) 179.2(9); N(3)−Pd(1)−Cl(2) 177.1(9); N(1)−Pd(1)−Cl(2) 92.8(9); Cl(1)−Pd(1)−Cl(2) 87.4(4). Angles between intersecting planes N(1)−N(2)−N(3)−N(4) and N(1)−Pd(1)−N(3) 158.1; N(1)−N(2)−N(3)−N(4) and N(2)−C(11)−N(4) 133.2; two heterocycle planes 126.8.

Scheme 2

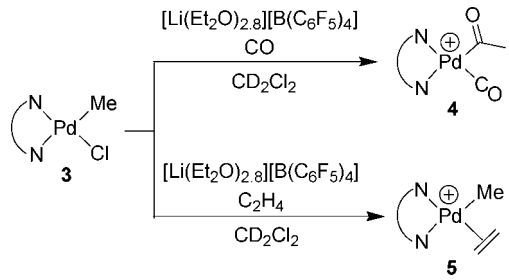

pz* resonances consistent with C_1 symmetry. As in **2**, fast rotation around the Si−CH and Si−tolyl bonds is observed.

Generation of a Pd Acyl Carbonyl Complex. The acyl carbonyl complex $\{(p\text{-tolyl})_3SiCH(pz^*)_2\}Pd\{C(=O)Me\}(CO)^+$ (**4**) was generated quantitatively by the reaction of **3** and $[Li(Et_2O)_{2.8}][B(C_6F_5)_4]$ in CD_2Cl_2 in the presence of CO (Scheme 2). The ^{13}C NMR spectrum of **4** at −60 °C in the presence of excess CO contains sharp resonances for bound CO (δ 171.3) and free CO (δ 184), indicating that intermolecular CO exchange is slow on the NMR time scale under these conditions.[3] The ν_{CO} value for the carbonyl ligand of **4** in CD_2Cl_2 solution is 2122 cm^{-1} (cf. free CO 2139 cm^{-1}), which indicates that **4** contains a moderately electrophilic Pd center. This value is lower than the values for $\{H_2C(pz)_2\}Pd\{C(=O)Me\}CO^+$ (2133 cm^{-1}) and $\{H_2C(pz^*)_2\}Pd\{C(=O)Me\}CO^+$ (2132 cm^{-1}),[1a] most likely due to the inductive and field effects of the –Si(*p*-tolyl)$_3$ group. For comparison, incorporation of a –C(*p*-tolyl)$_3$ group at the bridge position in a closely related system caused a smaller reduction in ν_{CO} (i.e., $\{(p\text{-tolyl})_3CCH(mim)_2\}Pd\{C(=O)Me\}CO^+$ (2118 cm^{-1}) vs $\{H_2C(mim)_2\}Pd\{C(=O)Me\}CO^+$ (2122 cm^{-1})).[1,4] Complex **4** decomposes to Pd^0 in a few hours at 25 °C.

Scheme 3

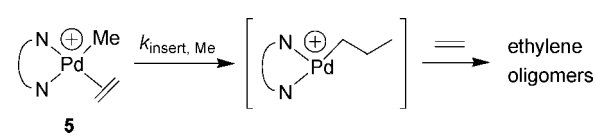

Generation of $\{(p\text{-tolyl})_3SiCH(pz^*)_2\}PdMe(C_2H_4)^+$. The methyl ethylene complex $[\{(p\text{-tolyl})_3SiCH(pz^*)_2\}PdMe(C_2H_4)][B(C_6F_5)_4]$ (**5**) was generated quantitatively by the reaction of **3** and $[Li(Et_2O)_{2.8}][B(C_6F_5)_4]$ in CD_2Cl_2 in the presence of ethylene at −60 °C (Scheme 2). Under these conditions insertion is not observed. The ^1H NMR spectrum of **5** at −60 °C contains two sharp sets of pz*-H4 resonances (δ 6.06, 5.85), consistent with C_1 symmetry. The Pd−Me resonance appears at δ 0.38, ca. 0.63 ppm downfield from the Pd−Me resonance of **3**. The ^1H NMR spectrum contains separate signals for bound (δ 4.15, 4.38) and free (δ 5.38) ethylene at −60 °C. Similarly, the ^{13}C spectrum contains separate resonances for bound (δ 87.5, br) and free (δ 130.0) ethylene. These data are consistent with slow exchange of bound and free ethylene and fast rotation around the Pd−(C_2H_4 centroid) axis in **5**.[5]

To probe the dynamics of Pd−(C_2H_4) rotation, **5** was generated in $CDCl_2F$ solution and low-temperature NMR spectra were recorded. At −120 °C, the ^1H NMR spectrum contains four broad signals (δ 5.21, 4.54, 4.26, 2.86) and the ^{13}C spectrum contains two broad signals (δ 83.6, 92.1) for the bound ethylene, indicating that ethylene rotation is slow on the chemical shift time scale at this temperature. The ^1H ethylene signals at δ 4.54 and 4.25 coalesce at −105 °C, from which the barrier to ethylene rotation was determined to be $\Delta G_{rot}^{\ddagger} = 8.2$ kcal mol^{-1}.

Kinetics of Ethylene Insertion of 5. In the presence of excess ethylene at −10 °C, **5** undergoes ethylene insertion to yield higher Pd−alkyl complexes and eventually ethylene oligomers (Scheme 3). The rate of insertion of **5** is first-order in Pd and zero-order in ethylene. The insertion rate constant, $k_{insert,Me} = 3.3(3) \times 10^{-3}$ s^{-1}, was determined by monitoring the disappearance of the Pd−Me ^1H NMR resonance. The insertion barrier is $\Delta G^{\ddagger} = 18.3$ kcal mol^{-1}. The $k_{insert,Me}$ value for **5** is greater than that for $\{Me_2C(pz)_2\}PdMe(C_2H_4)^+$ (2.2×10^{-4} s^{-1}), $\{H_2C(pz)_2\}PdMe(C_2H_4)^+$ (3.6×10^{-4} s^{-1}), and $\{H_2C(pz^*)_2\}PdMe(C_2H_4)^+$ (1.3×10^{-3} s^{-1}) at the same temperature.[1a,c] **5** undergoes ethylene insertion faster than any of the $\{bis(N\text{-heterocycle})methane\}Pd(R)(ethylene)^+$ species studied previously.[1]

Ethylene Oligomerization Behavior of $\{(p\text{-tolyl})_3SiCH(pz^*)_2\}PdMe^+$. Preparative scale ethylene oligomerizations were performed using **5** generated in situ by the reaction of **3** and $[Li(Et_2O)_{2.8}][B(C_6F_5)]$ in CH_2Cl_2 in the presence of ethylene. At −10 °C under 2.7 atm of ethylene, **5** produces a distribution of branched C_6–C_{20} internal olefins (Figure 2). Very little Pd^0 formation is observed under these conditions, indicating that

(2) (a) Minghetti, G.; Cinellu, M. A.; Bandini, A. L.; Banditelli, G.; Demartin, F.; Manassero, M. *J. Organomet. Chem.* **1986**, *315*, 387. (b) Burns, C. T.; Shen, H.; Jordan, R. F. *J. Organomet. Chem.* **2003**, *683*, 240. (c) Done, M. C.; Ruther, T.; Cavell, K. J.; Kilner, M.; Peacock, E. J.; Braussaud, N.; Skelton, B. W.; White, A. *J. Organomet. Chem.* **2000**, *607*, 78. (d) Newkome, G. R.; Gupta, V. K.; Theriot, K. J.; Ewing, J. C.; Wicelinski, S. P.; Huie, W. R.; Fronczek, F. R.; Watkins, S. F. *Acta Crystallogr., Sect. C: Cryst. Struct. Commun.* **1984**, *C40*, 1352. (e) Sanchez-Mendez, A.; de Jesus, E.; Flores, J. C.; Gomez-Sal, P. *Inorg. Chem.* **2007**, *46*, 4793.

(3) (a) For analogous compounds see: Wu, F.; Foley, S. R.; Burns, C. T.; Jordan, R. F. *J. Am. Chem. Soc.* **2005**, *127*, 1841. (b) Rix, F. C.; Brookhart, M. *J. Am. Chem. Soc.* **1996**, *118*, 6414.

(4) (a) Increasing the electron density at a remote position of a ligand lowered ν_{CO} in related complexes: Wu, F.; Jordan, R. F. *Organometallics* **2006**, *23*, 5631. (b) Lu, C. C.; Peters, J. C. *J. Am. Chem. Soc.* **2002**, *124*, 5272. (c) Thomas, J. C.; Peters, J. C. *J. Am. Chem. Soc.* **2001**, *123*, 5100.

(5) The four ethylene hydrogens comprise an ABCD system under slow rotation conditions, and an AA′BB′ system under fast rotation conditions.

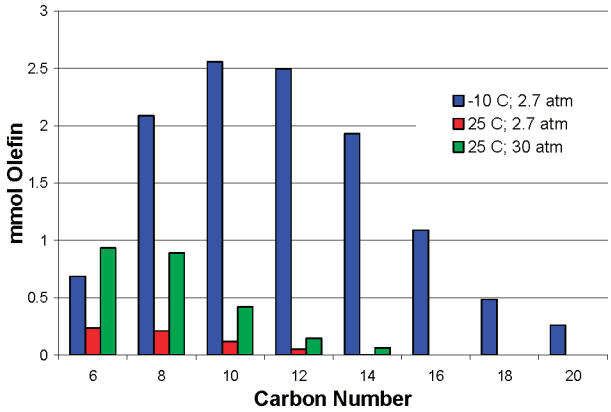

Figure 2. Distribution of olefins produced by **5**. Conditions: in situ generation of **5** from 30 μmol of **3** and 30 μmol of $[Li(Et_2O)_{2.8}][B(C_6F_5)]$ in 20 mL of CH_2Cl_2. Blue bars: −10 °C, 2.7 atm of ethylene; red bars: 25 °C, 2.7 atm of ethylene; green bars: 25 °C, 2.7 atm of ethylene.

catalyst decomposition is minimal. The turnover frequency (13×10^{-3} s^{-1}) is ca. 4 times higher than the ethylene insertion rate of **5**. At 25 °C under 2.7 atm of ethylene, **5** produces a distribution of branched C_6–C_{12} internal olefins (39 branches/10^3 C). The product distribution is very similar at 30 atm of ethylene pressure. Rapid formation of Pd^0 is observed during the 25 °C reactions, indicating that the catalyst is not stable at this temperature.[6]

To probe the nature of the decomposition process, a CH_2Cl_2 solution of **5** was exposed to ethylene (650 mm on demand) at 25 °C to model the oligomerization conditions. Pd^0 was recovered in 85% mass balance after 2 h. NMR and ESI-MS analysis of the product mixture showed that $[(p\text{-tolyl})_3SiCH(pz^*)_2]H^+$ was a major decomposition product, indicating that the ligand remains intact upon decomposition of the catalyst.[7]

Generation of [{(*p*-tolyl)$_3$SiCH(pz*)$_2$}PdCHMeCH$_2$-μ-H][B(C$_6$F$_5$)$_4$] (6). The reaction of **5** in $CDCl_2F$ at 0 °C in the absence of ethylene generates the β-H agostic isopropyl species $[\{(p\text{-tolyl})_3SiCH(pz^*)_2\}PdCHMeCH_2\text{-}\mu\text{-}H][B(C_6F_5)_4]$ (**6**) in 95% yield along with ca. 5% of higher β-agostic alkyl complexes (eq 1). Complex **6** is stable in $CDCl_2F$ solution below 0 °C.

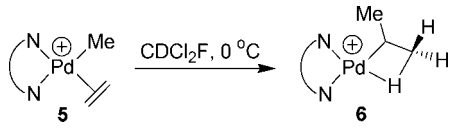

(1)

The ^1H NMR spectrum of **6** in $CDCl_2F$ at −115 °C contains a PdC*H*MeCH$_2$-μ-H resonance at δ 3.31, a nonagostic methyl resonance at δ 0.77, and PdCHMeC*H*$_2$-μ-H resonances at δ −0.04 and 0.81. The agostic β-H appears as a triplet at δ −8.91 ($^2J_{HH}$ = 18 Hz), which is characteristic of β-H agostic Pd−^{i}Pr species.[8] These assignments were confirmed by a COSY spectrum. Sharp singlets are observed for the (*p*-tolyl)$_3$SiC*H* (δ 6.45) and pz*-H4 (δ 6.05, 5.92) resonances.

At 0 °C, the ^1H NMR spectrum of **6** contains a broad signal at δ −2.10 for the isopropyl methyl hydrogens and a singlet at δ 3.09 for the PdC*H*MeCH$_2$-μ-H methine hydrogen. The spectrum also contains two sets of pz* resonances, showing that the sides of the N^N ligand remain inequivalent at this temperature. These results imply that in-place rotation around the Pd−C bond and concomitant exchange of agostic and nonagostic Me units is fast at 0 °C.[9]

Reaction of 6 with Ethylene. The reaction of **6** with 1 equiv of ethylene in CD_2Cl_2 at −80 °C results in partial reversible formation of the *n*-propyl ethylene species $[\{(p\text{-tolyl})_3SiCH(pz^*)_2\}Pd^nPr(C_2H_4)][B(C_6F_5)_4]$ (**7**, (eq 2)). Complex **7** is stable in CD_2Cl_2 solution up to −35 °C, at which temperature ethylene insertion occurs. The ^1H NMR spectrum of **7** in CD_2Cl_2 at −80 °C contains a broad resonance for the bound ethylene (δ 4.26)[10] and sharp singlets for the (*p*-tolyl)$_3$SiC*H* (δ 6.70) and pz*-H4 (δ 6.13, 5.90) hydrogens. The *n*-propyl resonances were identified with the aid of a COSY spectrum (−80 °C; PdC*H*$_2$CH$_2$CH$_3$: δ 1.72, 0.77; PdCH$_2$C*H*$_2$CH$_3$: δ 1.94; PdCH$_2$CH$_2$C*H*$_3$: δ 0.77).

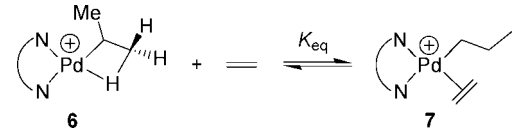

(2)

The dynamics of ethylene rotation of **7** were probed by low-temperature NMR in $CDCl_2F$ solution. At −115 °C, the ^1H NMR spectrum of **7** contains four resonances (δ 5.41, 4.54, 3.94, 2.83), and the ^{13}C NMR contains two resonances (δ 93.7, 86.1) for the bound ethylene, indicating slow rotation. The ^1H ethylene signals at δ 4.54 and 3.94 coalesce at −90 °C, giving $\Delta G_{rot}^{\ddagger}$ = 8.1 kcal mol^{-1}, similar to the value for **5**.

The equilibrium constant for ethylene coordination to **6** (eq 2), $K_{eq} = [\mathbf{7}][\mathbf{6}]^{-1}[C_2H_4]^{-1}$, was determined over the temperature range −80 to −35 °C by ^1H NMR using the characteristic (*p*-tolyl)$_3$SiC*H* resonances of **6** and **7**. At −80 °C, K_{eq} = 430 M^{-1}. Thermodynamic parameters for this equilibrium were determined by a van't Hoff analysis and are listed in Table 1. Extrapolation of the van't Hoff plot to –10 °C, the optimum ethylene oligomerization temperature, gives K_{eq} = 2.8 M^{-1}.

NMR Monitoring of the Reaction of 5 with Excess Ethylene. The **5**-catalyzed ethylene oligomerization reaction at −10 °C in CD_2Cl_2 was monitored by ^1H NMR by periodically cold-quenching the reaction and collecting ^1H NMR spectra at −80 °C. These spectra showed that a mixture of β-H agostic higher secondary alkyl complexes (**8**, R = distribution of alkyl groups) and alkyl ethylene complexes (**9**, R′ = distribution of alkyls groups) was present, as shown in Scheme 4. After the ethylene is consumed, the only Pd species in solution is **8**.

(6) The oligomerization distribution produced by **5** at 30 atm of ethylene fit a Shultz−Flory distribution (α = 0.35 and β = 1.8). However, oligomerizations at 2.7 atm of ethylene pressure did not produce Shultz−Flory distributions.

(7) The compound [**1**H][B(C$_6$F$_5$)$_4$] was generated quantitatively by the reaction of **1** (10 mg, 20 μmol) and $[H(OEt_2)_2][B(C_6F_5)_4]$ (16 mg, 20 μmol) in CD_2Cl_2 (0.7 mL) for 10 min at 25 °C. ^1H NMR (CD_2Cl_2, 25 °C): δ 12.63 (br s, 1H, H^+), 7.24 (m, 12 H, 4-Me-C$_6$*H*$_4$), 6.50 (s, 1H, CH), 6.06 (s, 2H, pz* H4), 2.39 (s, 9H, 4-*Me*-C$_6$H$_4$), 2.21 (s, 3H, pz* Me), 2.05 (s, 3H, pz* Me). ESI-MS: $[(pz^*)_2CHSi(p\text{-tolyl})_3]H^+$ calcd *m/z* 505.2, found 505.2. [**1**H][B(C$_6$F$_5$)$_4$] decomposes in CD_2Cl_2 solution at 25 °C (ca. 25% after 24 h).

(8) Tempel, D. J.; Brookhart, M. *Organometallics* **1997**, *17*, 2290.

(9) Two diastereomers are possible for **6**, which differ in the relative configurations of the N^N bridging carbon and the isopropyl methine carbon. Exchange of the agostic and nonagostic methyl groups by Pd−C bond rotation interconverts the diastereomers of **6**. However, only one set of resonances is observed for **6** at all temperatures. It is likely that the NMR spectra of the two diastereomers are very similar due to the remoteness of the two stereocenters.

(10) The broad resonance at δ 4.26 integrates for 4H and results from the overlap of the two resonances expected for the bound ethylene, which, based on the low-temperature limit spectrum, have very similar chemical shifts ($\Delta\delta$ = 0.12).

Table 1. Thermodynamic Parameters for Ethylene Coordination to {(*p*-tolyl)$_3$SiCH(pz*)$_2$}PdR$^+$ Species[a]

	6 (R = ^{i}Pr)[b,c]	**8** (R = alkyl)[d,e]
ΔH (kcal mol^{-1})	−7.4(5)	−5.8(3)
ΔS (cal mol^{-1} K^{-1})	−27(2)	−23(2)
ΔG_{293} (kcal mol^{-1})[f]	0.51	0.94
K_{eq} at −10 °C (M^{-1})[g]	2.8	0.72

[a] Determined in CD_2Cl_2 solution. [b] Coordination of ethylene to **6** gives the *n*-propyl ethylene complex **7**. [c] Based on NMR data in the temperature range −80 to −35 °C. [d] R = distribution of oligoethylene chains. [e] Based on NMR data in the temperature range −80 to −40 °C. [f] ΔG evaluated at 293 K. [g] K_{eq} = [(N^N)PdR(ethylene)$^+$]-[[(N^N)PdR$^+$]$^{-1}$[ethylene]$^{-1}$; determined by extrapolation of the van't Hoff plot.

Scheme 4

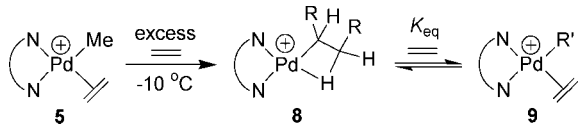

The ^{1}H NMR data for **8** are similar to those for isopropyl analogue **6**. The ^{1}H NMR chemical shifts (CD_2Cl_2, −80 °C) for the (*p*-tolyl)$_3$Si*CH* (δ 6.37), pz*-H4 (6.04, 5.93) and agostic β-H (δ −9.50, m) units of **8** are very similar to those for **6**.[11] The alkyl region of the ^{1}H spectrum of **8** was challenging to assign because a distribution of alkyl chain lengths is present (vide infra). However, the −80 °C COSY spectrum contains correlations between the β-H agostic, terminal β-H (δ 0.42, m), and α-methine signals (δ 3.03, m), and these signals integrate in a 1/1/1 ratio, confirming the β-H agostic secondary alkyl structure.[12]

The NMR data for **9** are similar to those for the *n*-propyl analogue **7**. The ^{1}H NMR chemical shifts (CD_2Cl_2, −80 °C) for the (*p*-tolyl)$_3$Si*CH* (δ 6.69), pz*-H4 (δ 6.08, 5.82), and bound ethylene (δ 4.15, br) units of **9** are very similar to those for **7**. The ^{1}H NMR spectrum of **9** in $CDCl_2F$ solution at −120 °C contains four ethylene signals (δ 4.45, 3.91, 3.57, 2.75). The δ 3.91 and 3.57 resonances coalesce at −90 °C, giving $\Delta G_{rot}^{\ddagger}$ = 8.3 kcal mol^{-1}, similar to the values for **5** and **7**.

The equilibrium constant for ethylene coordination to **8** (Scheme 4), K_{eq} = [**9**][**8**]$^{-1}$[C_2H_4]$^{-1}$, was determined by ^{1}H NMR from −80 to −40 °C, using the (*p*-tolyl)$_3$Si*CH* resonances for **8** and **9**. The thermodynamic parameters for this equilibrium are similar to the values for **6** and are listed in Table 1. K_{eq} is estimated to be 0.72 M^{-1} at −10 °C, slightly lower than the value for **6**.

Characterization of Alkyl Chain Length Distribution in 8. To determine alkyl chain length distribution in **8**, this species was reacted with CO and then NaOMe/MeOH to generate the corresponding distribution of methyl esters as shown in Scheme 5.[13] GC-MS analysis showed that a distribution of C_5 to C_{17} methyl esters formed. Multiple isomers were detected for each carbon number. These results are consistent with branching in the ethylene oligomers produced by **5** in Scheme 3.

Ethylene-*d*$_4$ Labeling Experiments. To confirm that **8** and **9** are involved in the catalytic ethylene oligomerization cycle,

Scheme 5

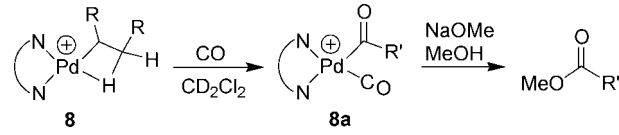

the reaction of **8** with ethylene-d_4 at −10 °C in CD_2Cl_2 was studied. The ^{1}H NMR spectrum (collected at −80 °C) showed that after 20 min at –10 °C the characteristic (*p*-tolyl)$_3$SiCH(pz*)$_2$ resonances for **8** and **9** were present, but the agostic β-H, terminal β-H, and methine C−H resonances of **8** and the ethylene resonance of **9** were absent. Upon subsequent reaction with unlabeled ethylene, the β-H agostic, terminal β-H, and methine C−H signals of **8** and the ethylene resonance of **9** appeared within 20 min. These results confirm that **8** and **9** are active growing species.

Catalyst Stability. The results above show that {(*p*-tolyl)$_3$SiCH(pz*)$_2$}PdR$^+$ species exist as an equilibrium mixture of **8** and **9** under catalytic ethylene oligomerization conditions. As noted above, fast catalyst decomposition to Pd^0 occurs in ethylene oligomerization at 25 °C. However, CD_2Cl_2 solutions of **8** are very stable at 25 °C (<10% decomposition after 2 days). Therefore, the low catalyst stability must result from instability of **9**.

Dynamic Properties of (N^N)Pd Complexes. The ^{1}H NMR spectrum of {(*p*-tolyl)$_3$SiCH(pz*)$_2$}Pd{C(=O)Me}(CO)$^+$ (**4**) at −60 °C contains two sharp sets of pz* signals, consistent with the expected inequivalence of the pz* units. However, the pz* resonances broaden and coalesce to one set as the temperature is raised; for example, the pz*-H4 signals coalesce at −40 °C as shown in Figure 3. In contrast, the (*p*-tolyl)$_3$Si*CH* and Pd{C(=O)*Me*} resonances remain sharp under these conditions. Similarly, the ^{13}C NMR spectrum of **4** exhibits broadening of the pz* resonances but not the (*p*-tolyl)$_3$Si*C*H or Pd{*C*(=O)*Me*} signals at −40 °C. The bound and free CO signals remain sharp at −40 °C, indicating that exchange of free and coordinated CO is slow.[14] These results show that **4** undergoes a dynamic process that exchanges the pz* units but does not involve the Pd{C(=O)Me} unit and does not involve intermolecular CO exchange (eq 3).[15]

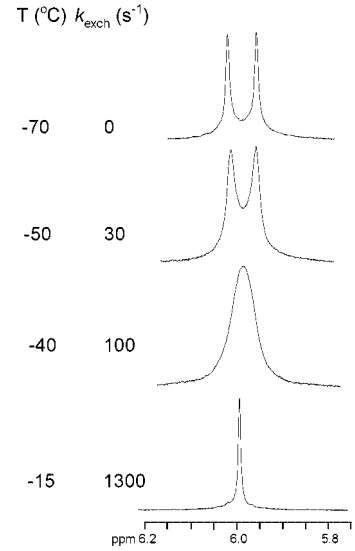

Figure 3. Variable-temperature ^{1}H NMR of **4** in CD_2Cl_2. The pz*-H4 region is shown. The first-order rate constants for the pz* exchange (k_{exch}) were determined by simulation of the observed spectra.

(11) Shultz, L. H.; Tempel, D. J.; Brookhart, M. *J. Am. Chem. Soc.* **2001**, *123*, 11539.

(12) The acetonitrile complex [{(*p*-tolyl)$_3$SiCH(pz*)$_2$}Pd(R)MeCN]-[$B(C_6F_5)_4$] **8b** was generated to probe the alkyl chain distribution. However, reaction of MeCN with **8** in CD_2Cl_2 at −10 °C yields an equilibrium mixture of **8** and **8b** (K_{eq} = [**8b**][**8**]$^{-1}$[MeCN]$^{-1}$ = 240 M^{-1}), from which little information about the alkyl chain distribution could be obtained.

(13) Liu, J.; Heaton, B. T.; Iggo, J. A.; Whyman, R. *Chem. Commun.* **2004**, 1326.

Table 2. Activation Parameters for pz* Site Exchange in {(*p*-tolyl)$_3$SiCH(pz*)$_2$}Pd Species Determined by Variable-Temperature NMR

complex	$\Delta G^{\ddagger}_{293}$[a] (kcal mol^{-1})	$\Delta H^{\ddagger}$ (kcal mol^{-1})	$\Delta S^{\ddagger}$ (cal mol^{-1} K^{-1})
3	17.8	21.7(6)	13(2)
4	11.0	9.2(3)	−6(2)
6	15.4		
7	11.4	7.2(4)	−14(2)
9	11.3	8.5(4)	−9(2)

[a] $\Delta G^{\ddagger}$ evaluated at 293 K.

Activation parameters for the exchange were obtained from the variable-temperature ^{1}H NMR spectra and are listed in Table 2. Complex **8a** (Scheme 5), which contains a distribution of alkyl chains, also undergoes fast pz* site exchange.[16]

The alkyl ethylene complexes **7** and **9** also display selective

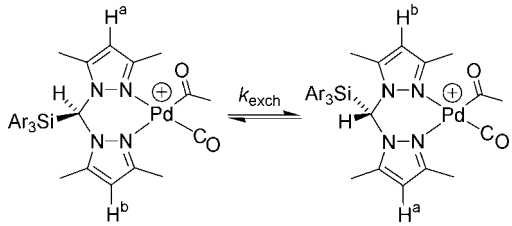

4, Ar = *p*-tol (3)

broadening of the pz* signals, even at −80 °C, indicating that pz* exchange is fast in these cases. The activation parameters for pz* exchange for **7** and **9** are listed in Table 2 and are similar to those for **4**. The rate of pz* exchange in **7** and **9** is independent of ethylene concentration over a wide range (**7**: 10–140 mM; **9**; 70–1340 mM). Therefore, pz* exchange cannot be explained by intermolecular ethylene exchange.

In contrast, the other {(*p*-tolyl)$_3$SiCH(pz*)$_2$}Pd species studied here undergo much slower (or no) pz* exchange. The ^{1}H NMR spectrum of **3** (in 1,1,2,2-tetrachloroethane-d_2) contains two sharp sets of pz* signals at 25 °C, but these resonances broaden as the temperature is raised, showing that slow pz* exchange occurs. Activation parameters for pz* exchange of **3** were determined from the coalescence of the pz*-H4 resonances (δ 5.92, 5.58) and are listed in Table 2. The pz* exchange barrier for **3**, $\Delta G^{\ddagger}_{298} = 17.8$ kcal mol^{-1}, is much higher than those for **4**, **7**, and **9**. EXSY spectra of **3** at 20 °C confirm that pz* exchange occurs and show that the barrier is similar in CD_2Cl_2 ($\Delta G^{\ddagger}_{293} = 17.7$ kcal mol^{-1}) and THF-d_8 (17.9 kcal mol^{-1}). The absence of a significant solvent dependence of the barrier suggests that solvent coordination does not play a critical role in the pz* exchange of **3**. Similarly, the ^{1}H NMR spectra of **8** (at 25 °C) and **5** (up to −40 °C; insertion occurs above this temperature) contain two sharp sets of pz* signals characteristic of slow pz* exchange.

Complex **6** undergoes pz* exchange at an intermediate rate. The ^{1}H NMR spectra of **6** exhibit two sharp sets of pz* signals up to 0 °C, but these resonances are selectively broadened at 20 °C. The barrier to pz* exchange estimated from the excess line width is $\Delta G^{\ddagger}_{298} = 15.4$ kcal mol^{-1} (Table 2).[17]

Scheme 6

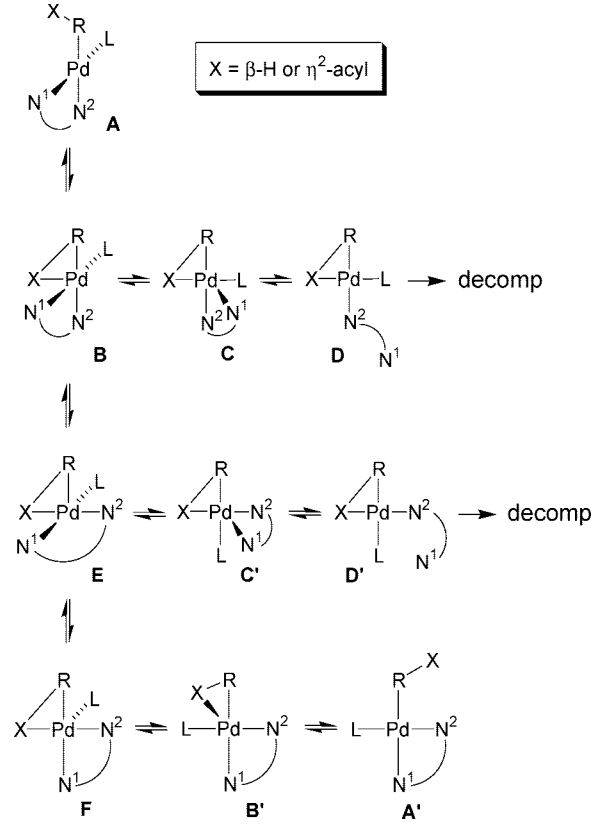

Mechanism of Pz* Exchange and Relationship to Catalyst Stability. Interestingly, there is a qualitative correlation between the thermal stability and the barriers to pz* site exchange of {(*p*-tolyl)$_3$SiCH(pz*)$_2$}Pd species. Complexes **3** and **8** are very stable at 25 °C and exhibit very slow pz* site exchange, while **4** and **9** are unstable at 25 °C and exhibit fast pz* exchange rates. A common feature of the unstable, fast-pz*-exchange species is that they contain a possible internal donor (either η^2-acyl or agostic β-H),[18] while the more stable, slow-pz*-exchange species do not. These considerations suggest that catalyst decomposition and pz* exchange both involve initial coordination of the internal donor. A reasonable mechanism that explains catalyst decomposition and pz* exchange is shown in Scheme 6.

The key feature of Scheme 6 is the formation of a configurationally labile five-coordinate intermediate **B** by coordination of the internal donor X (β-H agostic or η^2-acyl). **B** can isomerize (via trigonal bipyramidal intermediates that are not shown) to **C**, which contains a pz* ligand in the axial site from which it can dissociate (**D**), ultimately leading to loss of the N^N ligand and decomposition. **B** can also isomerize to **E** and then **C′**, leading to decomposition. Alternatively, **E** can isomerize to **F** and then **B′**, ultimately resulting in pz* exchange (**A′**). A more complete mechanism showing the trigonal bipyramidal intermediates is given in the Supporting Information.

(14) Even if intermolecular CO exchange were fast on the NMR time scale, the pz* site exchange would not be explained since associative CO exchange is expected to be stereospecific.

(15) A similar exchange process was noted for $H_2C(pz)_2Pd\{C(=O)Me\}CO^+$ and $H_2C(3,5\text{-}Me_2\text{-}pz)_2Pd\{C(=O)Me\}CO^+$ but was not studied in detail. See ref 1a.

(16) The ^{1}H NMR spectrum of **8a** contains one broad resonance for the two pz*-H4 hydrogens at–40 °C. The ^{13}C NMR pz* resonances are broadened into the baseline and the bound and free CO resonances are sharp at–40 °C. The results show that pz* exchange is fast on the NMR time scale and does not involve intermolecular CO exchange at −40 °C.

(17) For **6** at 20 °C, the excess linewidth of the pz*-H4/H4′ resonance is $\Delta\omega_{1/2} = 6$ Hz (relative to the (*p*-tolyl)$_3$Si*CH* resonance), and $k_{exch} = \pi\Delta\omega_{1/2} = 19$ s^{-1}.

(18) (a) Shultz, C. S.; DeSimone, J. M.; Brookhart, M. *J. Am. Chem. Soc.* **2001**, *123*, 9172. (b) Margl, P.; Ziegler, T. *J. Am. Chem. Soc.* **1996**, *118*, 7337. (c) Svensson, M.; Matsubara, T.; Morokuma, K. *Organometallics* **1996**, *15*, 5568.

Scheme 7

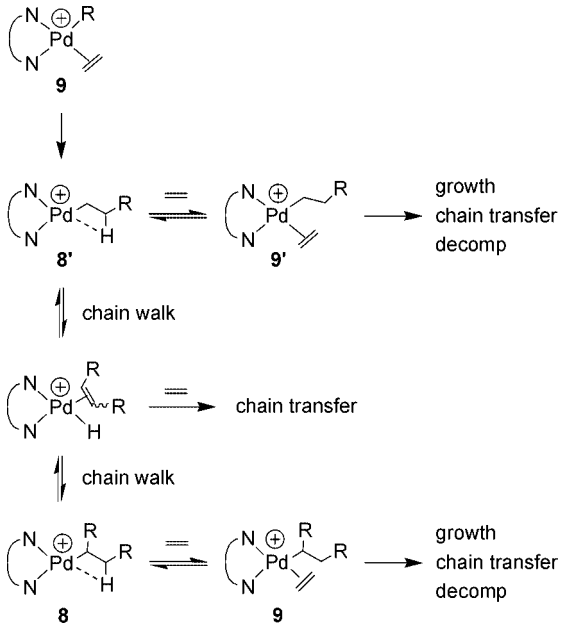

Mechanism of Ethylene Oligomerization. The key observations pertaining to the mechanism of ethylene oligomerization by **5** are as follows: (i) **5** produces a distribution of branched internal olefins, (ii) the oligomer distribution is essentially independent of ethylene pressure, (iii) an equilibrium mixture of β-H agostic species **8** and ethylene adducts **9** is present under catalytic conditions, (iv) catalyst deactivation occurs rapidly at 25 °C with loss of the N^N ligand, and (v) **8** is stable at 25 °C, while **9** is unstable at 25 °C. A mechanism that is consistent with these results is shown in Scheme 7. The alkyl ethylene complex **9** undergoes insertion to generate the primary alkyl species **8′**. Species **8′** either is trapped by ethylene to yield a primary alkyl ethylene adduct **9′** or chain walks to generate a secondary alkyl species (**8**) and the corresponding ethylene adduct **9**. Species **9** and **9′** insert, resulting in chain growth, or decompose as described above. Chain transfer occurs by ethylene displacement of olefin from the $(N^N)Pd(H)(olefin)^+$ chain-walk intermediates, or by β-H transfer to coordinated ethylene in **9** or **9′**.

Conclusion

The $\{(p\text{-tolyl})_3SiCH(pz^*)_2\}Pd(Me)(ethylene)^+$ cation (**5**) catalytically oligomerizes ethylene to branched C_6–C_{20} internal olefins. NMR studies show that an equilibrium mixture of base-free β-agostic secondary alkyl $(N^N)PdR^+$ species (**8**) and ethylene adducts $(N^N)Pd(R)(ethylene)^+$ (**9**) is present under oligomerization conditions. At 20 °C, **9** undergoes fast site exchange of the pz* rings and decomposes readily to Pd^0, while **8** does not undergo pz* site exchange and is stable. It is proposed that the decomposition and pz* exchange of **9** both involve initial coordination of a β-H to generate a configurationally labile five-coordinate intermediate, which can isomerize, resulting in pz* site exchange or displacement of one arm of the N^N ligand.

Experimental Section

General Considerations. All manipulations were performed using glovebox or Schlenk techniques under purified N_2. Nitrogen was purified by passage through columns containing activated molecular sieves and Q-5 oxygen scavenger. Pentane, hexanes, toluene, and benzene were purified by passage through columns of activated alumina and BASF R3-11 oxygen scavenger. Diethyl ether and tetrahydrofuran were distilled from Na/benzophenone ketyl. Dichloromethane was distilled from P_2O_5. $Cl_2DCCDCl_2$, $CDCl_3$, and CD_2Cl_2 were distilled from CaH_2 or P_2O_5. $CDCl_2F$ was prepared according to the literature and distilled from P_2O_5.[19] CO was purchased from Aldrich and used as received. Ethylene (research grade) was obtained from Matheson and used as received. $[Li(Et_2O)_{2.8}][B(C_6F_5)_4]$ was obtained from Boulder Scientific and used as received. The Et_2O content of the $[Li(Et_2O)_{2.8}][B(C_6F_5)_4]$ salt was determined by ^1H NMR with C_6Me_6 as an internal standard. $(MeCN)_2PdCl_2$ was obtained from Strem and used as received. The compounds $(pz^*)_2CH_2$ (pz^* = 3,5-Me_2-pyrazole),[20] (p-tolyl)$_3$SiCl,[21] (p-tolyl)$_3SiOSO_2CF_3$,[22] and (cod)Pd(Me)Cl[23] were prepared as described in the literature. All other chemicals were purchased from standard suppliers and used without further purification.

Elemental analyses were performed by Midwest Microlabs (Indianapolis, IN). Infrared spectra were obtained at 25 °C under an N_2 atmosphere using a Nicolet NEXUS 470 FT-IR spectrometer. GC-MS analyses were performed on a HP-6890 instrument equipped with a HP-5973 mass selective detector.

NMR spectra were recorded in Teflon-valved NMR tubes on Bruker DRX-400 or -500 spectrometers at ambient probe temperature unless otherwise indicated. ^1H and ^{13}C chemical shifts are reported versus $SiMe_4$ and were determined by reference to the residual solvent peaks. ^{19}F and ^{11}B chemical shifts were referenced to external neat $CFCl_3$ and $BF_3 \cdot Et_2O$, respectively. Coupling constants are reported in Hz. NMR probe temperatures were calibrated by a MeOH thermometer.[24] For variable-temperature NMR experiments, the probe was maintained at a given temperature for 20–30 min to allow the sample to reach thermal equilibrium.

The NMR spectra of cationic Pd compounds contain signals of the free $B(C_6F_5)_4^-$ anion. $^{13}C\{^1H\}$ NMR (CD_2Cl_2, −60 °C): δ 147.5 (dm, J = 241, C2), 137.8 (dm, J = 238, C4), 135.8 (dm, J = 249, C3), 123.6 (br, C1). ^{11}B NMR (CD_2Cl_2, −60 °C): δ −16.9 (s). ^{19}F NMR (CD_2Cl_2, −60 °C): δ −133.7 (br s, 2F, o-F), −163.0 (t, J = 23, 1F, p-F), −167.0 (t, J = 19, 2F, m-F). Solutions of cationic species generated in situ from the reaction of **2** and $[Li(Et_2O)_{2.8}][B(C_6F_5)_4]$ contain LiCl and free Et_2O. In some experiments the Et_2O was used as an internal standard in NMR experiments.

$(pz^*)_2$CHSi(p-tolyl)$_3$ (1). A solution of $(3,5\text{-}Me_2\text{-}pz)_2CH_2$ (0.727 g, 3.56 mmol) in THF (75 mL) was cooled to −78 °C, and ^{n}BuLi (2.66 M in hexanes, 1.40 mL, 3.74 mmol) was added over 5 min while the mixture was stirred. A white precipitate formed. The mixture was stirred at −78 °C for 1 h. A solution of (p-tolyl)$_3$SiOTf (1.68 g, 3.74 mmol) in THF (30 mL) cooled to −78 °C was added by cannula. The resulting yellow solution was stirred at −78 °C for 2 h, allowed to warm to 25 °C, and stirred for 12 h. The yellow mixture was quenched with saturated aqueous NH_4Cl (150 mL) and extracted with CH_2Cl_2 (3 × 75 mL). The clear yellow CH_2Cl_2 extract was washed with aqueous 10% Na_2CO_3 (200 mL), saturated aqueous $NaHCO_3$ (200 mL), and H_2O (200 mL) and finally dried over $MgSO_4$. The solvent

(19) Siegel, J. S.; Anet, F. A. L. *J. Org. Chem.* **1988**, *53*, 2629.
(20) Joshi, V. S.; Sarkar, A.; Rajamohanan, P. R. *J. Organomet. Chem.* **1991**, *409*, 341.
(21) Bassindale, A. R.; Ellis, R. J.; Taylor, P. G. *J. Chem. Res., Synop.* **1996**, 34.
(22) Asadi, A.; Avent, A. G.; Eaborn, C.; Hill, M. S.; Hitchcock, P. B.; Meehan, M. M.; Smith, J. D. *Organometallics* **2002**, *21*, 2183.
(23) Rülke, R. E.; Ernsting, J. M.; Spek, A. L.; Elsevier, C. J.; van Leeuwen, P. W. N. M.; Vrieze, K. *Inorg. Chem.* **1993**, *32*, 5769.
(24) Van Geet, A. L. *Anal. Chem.* **1970**, *42*, 679.

was removed under vacuum. The resulting white solid was purified by column chromatography using neutral alumina, eluting with pentane (150 mL) and then pentane/CH_2Cl_2 (1:1 v/v, 150 mL). The second fraction was dried over $MgSO_4$ and taken to dryness under vacuum to afford a white solid (1.38 g, 77%). ^{1}H NMR ($CDCl_3$): δ 7.38 (m, 6H, 4-Me-C_6H_4), 7.07 (m, 6H, 4-Me-C_6H_4), 6.64 (s, 1H, CH), 5.68 (s, 2H, pz* H4), 2.31 (s, 9H, 4-*Me*-C_6H_4) 2.08 (s, 6H, pz*-Me), 1.78 (s, 6H, pz*-Me). ^{13}C{^{1}H} NMR ($CDCl_3$): δ 146.3, 140.1, 139.2, 136.8, 128.9, 128.2, 106.4, 67.8, 21.5, 13.4, 10.9. Anal. Calcd for $C_{32}H_{36}N_4Si$: C, 76.15; H, 7.19; N, 11.10. Found: C, 75.76; H, 7.27; N, 10.57.

{(*p*-tolyl)$_3$SiCH(pz*)$_2$}PdCl$_2$ (2). A solution of $(MeCN)_2PdCl_2$ (0.259 g, 1.00 mmol) and (3,5-Me_2-pz)$_2$CHSi(*p*-tolyl)$_3$ (0.530 g, 1.05 mmol) in CH_2Cl_2 (25 mL) was stirred for 2 h at 25 °C. The orange solution was taken to dryness under vacuum. The resulting orange solid was suspended in Et_2O (25 mL), stirred for 30 min, and collected by filtration. The solid was washed with pentane (20 mL) and dried under vacuum to yield **2** as an orange powder (0.587 g, 86%). ^{1}H NMR ($CDCl_3$): δ 7.45 (m, 6H, 4-Me-C_6H_4), 7.18 (m, 6H, 4-Me-C_6H_4), 6.58 (s, 1H, CH), 5.77 (s, 2H, pz* H4), 2.54 (s, 6H, pz* 5-Me), 2.35 (s, 9H, 4-*Me*-C_6H_4), 1.96 (s, 6H, pz* 3-Me). ^{13}C{^{1}H} NMR ($CDCl_3$): δ 153.9, 141.3, 140.4, 137.0, 129.5, 125.0, 108.0, 65.4, 21.7, 15.6, 11.7. Anal. Calcd for $C_{32}H_{36}Cl_2N_4PdSi$: C, 56.35; H, 5.32; N, 8.21. Found: C, 56.40; H, 5.31; N, 8.10.

{(*p*-tolyl)$_3$SiCH(pz*)$_2$}PdMeCl (3). A flask was charged with (cod)PdMeCl (0.265 g, 1.00 mmol) and (3,5-Me_2-pz)$_2$CHSi(*p*-tolyl)$_3$ (0.510 g, 1.01 mmol), and Et_2O (15 mL) was added by syringe at 25 °C. A white precipitate formed rapidly. The mixture was stirred at 25 °C for 4 h, and the solid was collected by filtration. The solid was washed with Et_2O (2 × 10 mL), washed with pentane (10 mL), and dried under vacuum to yield a white solid (0.499 g, 75%). The isolated solid contained 0.12 equiv of Et_2O, which was quantified by ^{1}H NMR. ^{1}H NMR (CD_2Cl_2): δ 7.34 (m, 6H, 4-Me-C_6H_4), 7.14 (m, 6H, 4-Me-C_6H_4), 6.58 (s, 1H, CH), 5.92 (s, 1H, pz* H4/H4′), 5.63 (s, 1H, pz* H4/H4′), 2.38 (s, 3H, pz* Me), 2.30 (s, 9H, 4-*Me*-C_6H_4), 2.15 (s, 3H, pz* Me), 2.15 (s, 3H, pz* Me), 1.92 (s, 3H, pz* Me), −0.25 (s, 3H, PdMe). ^{13}C{^{1}H} NMR (CD_2Cl_2): δ 151.0 (3/3′-pz*), 150.4 (3/3′-pz*), 140.5, 140.2 (5/5′-pz*), 138.6 (5/5′-pz*), 136.5, 128.7, 126.0, 107.0 (4/4′-pz*), 106.0 (4/4′-pz*), 63.3 (CH), 21.2 (4-*Me*-C_6H_4), 14.9 (pz* Me), 13.6, (pz* Me), 11.7 (pz* Me), 11.6 (pz* Me), −6.5 (PdMe). Anal. Calcd for $C_{33}H_{39}ClN_4PdSi \cdot 0.12Et_2O$: C, 59.97; H, 5.99; N, 8.36. Found: C, 59.70; H, 6.05; N, 8.35.

Generation of [{(*p*-tolyl)$_3$SiCH(pz*)$_2$}Pd{C(=O)Me}(CO)][B(C$_6$F$_5$)$_4$] (4). A valved NMR tube containing a CD_2Cl_2 (0.7 mL) solution of **2** (0.020 g, 0.030 mmol) and $[Li(Et_2O)_{2.8}][B(C_6F_5)_4]$ (0.027 g, 0.030 mmol) was cooled to −196 °C and exposed to CO (1 atm) for 5 min The tube was sealed and warmed to −78 °C. The tube was briefly warmed to 23 °C and vigorously shaken. A slurry of a white solid in a colorless supernatant was obtained. The tube was kept at −78 °C and transferred to a precooled (−60 °C) NMR probe, and NMR spectra were recorded. The ^{1}H NMR spectrum established that **4** had formed (100% vs Et_2O). ^{1}H NMR (CD_2Cl_2, −60 °C): δ 7.22 (m, 6H, 4-Me-C_6H_4), 7.17 (m, 6H, 4-Me-C_6H_4), 6.50 (s, 1H, CH), 6.00 (s, 1H, pz* H4/H4′), 5.92 (s, 1H, pz* H4/H4′), 2.60 (s, 3H, CO*Me*), 2.34 (s, 9H, 4-*Me*-C_6H_4), 2.18 (s, 3H, pz* Me), 2.12 (s, 3H, pz* Me), 2.09 (s, 3H, pz* Me), 1.77 (s, 3H, pz* Me). ^{13}C{^{1}H} NMR (CD_2Cl_2, −60 °C): δ 210.7 (*C*(O)Me), 171.3 (Pd*C*O), 151.8 (3/3′-pz*), 150.6 (3/3′-pz*), 142.9 (5/5′-pz*), 142.3, 141.9 (5/5′-pz*), 137.0, 129.3, 123.5, 108.2 (4/4′-pz*), 107.7 (4/4′-pz*), 63.1 (CH), 43.7 (CO*Me*), 21.5 (4-*Me*-C_6H_4), 15.3, 14.4, 11.8, 11.2; the free CO resonance appears at δ 184.3. IR (CD_2Cl_2, cm^{-1}): 2122 (ν_{CO}), 1746 (ν_{acyl}).

Generation of [{(*p*-tolyl)$_3$Si)CH(pz*)$_2$}PdMe(H$_2$C=CH$_2$)][B(C$_6$F$_5$)$_4$] (5). A valved NMR tube containing a CD_2Cl_2 (0.7 mL) solution of **2** (0.013 g, 0.020 mmol) and $[Li(Et_2O)_{2.8}][B(C_6F_5)_4]$ (0.018 g, 0.020 mmol) was cooled to −196 °C, and ethylene (0.18 mmol) was added by vacuum transfer. The tube was sealed, warmed to −78 °C, and transferred to a precooled (−60 °C) NMR probe, and NMR spectra were recorded at −60 °C. The ^{1}H NMR spectrum established that **5** had formed (100% vs Et_2O after 20 min). Under these conditions (−60 °C), exchange of coordinated and free ethylene is slow, but rotation of the bound ethylene is fast on the NMR chemical shift time scale. ^{1}H NMR (CD_2Cl_2, −60 °C): δ 7.21 (m, 6H, 4-Me-C_6H_4), 7.06 (m, 6H, 4-Me-C_6H_4), 6.59 (s, 1H, CH), 6.06 (s, 1H, pz* H4/H4′), 5.85 (s, 1H, pz* H4/H4′), 4.38 (m, 2H, H_2C=CH_2), 4.15 (br m, 2H, H_2C=CH_2), 2.34 (s, 9H, 4-*Me*-C_6H_4), 2.32 (s, 3H, pz* Me), 2.07 (s, 3H, pz* Me), 2.04 (s, 3H, pz* Me), 1.82 (s, 3H, pz* Me), 0.38 (s, 3H, PdMe). ^{13}C{^{1}H} NMR (CD_2Cl_2, −60 °C): δ 151.5 (3/3′-pz*), 150.6 (3/3′-pz*), 142.0 (5/5′-pz*), 141.9, 141.1 (5/5′-pz*), 136.2, 129.3, 124.1, 108.2 (4/4′-pz*), 108.1 (4/4′-pz*), 87.5 (br, H_2C=CH_2), 63.3 (CH), 21.3 (4-*Me*-C_6H_4), 14.9, 12.6, 11.7, 11.3, 7.0 (PdMe). A solution of **5** in $CDCl_2F$ was generated as described above and analyzed by variable-temperature (−60 °C to −120 °C) NMR. ^{1}H NMR ($CDCl_2F$, −120 °C): δ 5.21 (br m, H_2C=CH_2), 4.54 (br m, H_2C=CH_2), 4.26 (br m, H_2C=CH_2), 2.86 (br m, H_2C=CH_2). ^{13}C{^{1}H} ($CDCl_2F$, −120 °C) δ 92.1 (br, H_2C=CH_2), 83.6 (br, H_2C=CH_2).[25] The rotational barrier $\Delta G^{\ddagger}_{rot}$ = 8.2 kcal mol^{-1} was obtained from the coalescence of the δ 4.54 and 4.26 resonances, using the coalescence approximation ($k = \pi(\nu_a - \nu_b)/2^{1/2}$; k_{rot} = 310 s^{-1} at $T_{coalescence}$ = −105 °C).[26]

Kinetics of Insertion of [{(*p*-tolyl)$_3$Si)CH(pz*)$_2$}PdMe(H$_2$C=CH$_2$)][B(C$_6$F$_5$)$_4$] (5). A CD_2Cl_2 solution of **5** containing free ethylene (280 mM) was generated in a valved NMR tube as described above and maintained at −10 °C. Periodically the tube was cold-quenched in a −78 °C bath for 5 min and transferred to a precooled (−60 °C) NMR probe, where a ^{1}H NMR spectrum was recorded. Values of $I_{0,PdMe}$, I_{PdMe}, and I_{Et2O} where $I_{0,PdMe}$ = the integral of the Pd−Me resonance of **5** at the start of the experiment, I_{PdMe} = the integral of the Pd−Me resonance at time point, and I_{Et2O} = the integral of the Et_2O internal standard, were obtained. A plot of $\ln(A_{PdMe}/A_{0,PdMe})$, where $A_{PdMe} = I_{PdMe}/I_{Et2O}$ and $A_{0,PdMe} = I_{0,PdMe}/I_{Et2O}$, versus time was linear (r^2 = 0.996). The slope of the line equals $-k_{insert,Me}$. For **5**, $k_{insert,Me}$ = 3.3(3) × 10^{-3} s^{-1} at −10 °C (~3 half-lives). An identical result was obtained for [free H_2C=CH_2] = 110 mM, which shows that the insertion rate is zero-order in ethylene.

Low-Pressure Oligomerization of Ethylene by [{(*p*-tolyl)$_3$SiCH(pz*)$_2$}PdMe(H$_2$C=CH$_2$)][B(C$_6$F$_5$)$_4$] (5). A 200 mL Fischer-Porter bottle equipped with a magnetic stir bar was charged with **2** (0.020 g, 0.030 mmol) and $[Li(Et_2O)_{2.8}][B(C_6F_5)_4]$ (0.027 g, 0.030 mmol). The bottle was attached to a stainless steel double-manifold vacuum/ethylene line, placed under vacuum to remove the nitrogen atmosphere, and then charged with ethylene (3 atm). The bottle was cooled (−78 °C) and vented to decrease the ethylene pressure to 1 atm, and CH_2Cl_2 (20 mL) was added by syringe. The ethylene pressure was immediately

(25) The pz* and (*p*-tolyl)$_3$SiCH resonances do not shift or broaden significantly due to temperature or solvent.

(26) The other two ethylene ^{1}H NMR resonances (δ 5.42, 2.86) were broadened into the baseline at −105 °C.

increased 3 atm, and the solution was warmed to the desired temperature and stirred for 18 h, during which time the total pressure was kept constant (3 atm) by feeding ethylene on demand. The ethylene feed was turned off and the reactor was vented. In the −10 °C experiments, the product mixture was a slurry of a white solid in a pale yellow supernatant. In the room-temperature experiments, the product mixture was a slurry of a black solid in a yellow supernatant. Toluene (50 μL, for use as an internal standard) was added when the pressure reached 1 atm. An aliquot (ca. 200 μL) of the mixture was filtered through a small pad of silica with 2-methylbutane (3 mL) as the eluent. The filtrate was analyzed by quantitative GC-MS to determine the oligomer distribution. A solution of HCl in MeOH (1 M, 5 mL) was added to the remainder of the mixture, and the mixture was taken to dryness under vacuum. The residue was taken up in hexanes (20 mL) and filtered through a plug of silica gel. The solvent was removed under vacuum to afford a mixture of C_{12}–C_{20} oligomers, which was characterized by GC-MS. ^{1}H NMR ($CDCl_3$): δ 5.36 (m, R*H*C═C*H*R′), 5.08 (br s, RR′C═C*H*R″), 1.98 (m, allylic H), 1.60 (*H*$_3$CRC═CR′R″), 1.25 (C*H*$_2$, C*H*), 0.83 (m, C*H*$_3$). The branch number (39 branches/10^3 C) carbons was determined by ^{1}H NMR.[27,28]

High-Pressure Oligomerization of Ethylene by [{(*p*-tolyl)$_3$SiCH(pz*)$_2$}PdMe(H$_2$C═CH$_2$)][B(C$_6$F$_5$)$_4$] (5). An autoclave was charged with **2** (0.020 g, 0.030 mmol) and [Li(Et$_2$O)$_{2.8}$][B(C$_6$F$_5$)$_4$] (0.027 g, 0.030 mmol), CH_2Cl_2 (20 mL) was added by syringe, and the autoclave was pressurized with ethylene (30 atm) that was fed on demand. The mixture was stirred for 18 h at 25 °C. The autoclave was vented and toluene (50 μL, for use as an internal standard) was added when the pressure reached 1 atm. The product mixture was a slurry of a black solid in a yellow supernatant. An aliquot (ca. 200 μL) of the mixture was filtered through a small pad of silica with 2-methylbutane (3 mL) as the eluent. This solution was analyzed by quantitative GC-MS to determine the oligomer distribution. A solution of HCl in MeOH (1 M, 5 mL) was added to the remainder of the mixture, and the mixture was taken to dryness under vacuum. The residue was taken up in hexanes (20 mL) and filtered through a plug of silica gel. The solvent was removed under vacuum to afford a mixture of C_{12}–C_{20} oligomers (0.045 g), which was characterized by GC-MS.

Generation of [{(*p*-tolyl)$_3$SiCH(pz*)$_2$}PdCHMeCH$_2$-μ-H][B(C$_6$F$_5$)$_4$] (6). A valved NMR tube containing a $CDCl_2F$ (0.6 mL) solution of **2** (13 mg, 0.020 mmol) and [Li(Et$_2$O)$_{2.8}$][B(C$_6$F$_5$)$_4$] (18 mg, 0.020 mmol) was cooled to −196 °C, and ethylene (0.020 mmol) was added by vacuum transfer. The solution was thawed at −78 °C, warmed to 0 °C for 30 min, cooled to −78 °C, and transferred to a precooled (−115 °C) NMR probe, and NMR spectra were recorded. The NMR spectra established that **6** had formed (100% vs Et_2O). ^{1}H NMR ($CDCl_2F$, −115 °C): δ 7.27–7.15 (br m, 12H, 4-Me-C$_6$*H*$_4$), 6.45 (s, 1H, CH), 6.05 (s, 1H, pz* H4/H4′), 5.92 (s, 1H, pz* H4/H4′), 3.31 (m, 1H, PdC*H*MeCH$_2$-μ-H), 2.35 (s, 9H, 4-*Me*-C$_6$H$_4$), 2.31 (s, 3H, pz* Me), 2.19 (s, 3H, pz* Me), 2.11 (s, 3H, pz* Me), 1.71 (s, 3H, pz* Me), 0.85 (m, 1H, PdCHMeC*H*$_2$-μ-H), 0.77 (d, J = 6 Hz, 3H, PdCH*Me*CH$_2$-μ-H), −0.04 (m, 1H, PdCHMeC*H*$_2$-μ-H), −8.91 (t, J = 18 Hz, 1H, PdCHMeCH$_2$-μ-*H*). ^{13}C{^{1}H} NMR ($CDCl_2F$, −115 °C): δ 151.8 (3/3′-pz*), 149.5 (3/3′-pz*), 142.6 (5/5′-pz*), 141.9 (5/5′-pz*), 140.9, 136.9, 129.3, 124.3, 108.0 (4/4′-pz*), 106.7 (4/4′-pz*), 63.3 (CH), 43.9 (Pd*C*HMeCH$_2$-μ-H), 21.3 (4-*Me*-C$_6$H$_4$), 20.7 (PdCH*Me*CH$_2$-μ-H), 14.7, 14.3, 14.2 (br s, PdCHMe*C*H$_2$-μ-H), 11.7, 10.8. Key ^{1}H–^{1}H COSY correlations ($CDCl_2F$, −115 °C): δ 3.31 (PdC*H*MeCH$_2$-μ-H) coupled to δ 0.85 (PdCHMeC*H*$_2$-μ-H), 0.77 (PdCH*Me*CH$_2$-μ-H), and 0.04 (PdCHMeC*H*$_2$-μ-H); δ 0.85 (PdCHMeC*H*$_2$-μ-H) coupled to δ 0.04 (PdCHMeC*H*$_2$-μ-H); δ 0.85 and 0.04 (PdCHMeC*H*$_2$-μ-H) coupled to δ 0.77 (PdCH*Me*CH$_2$-μ-H) and δ −8.90 (PdCHMeCH$_2$-μ-*H*). The solution of **6** in $CDCl_2F$ was warmed to 0 °C, and broadening of the PdCH*Me*C*H*$_2$-μ-*H* resonances was observed. ^{1}H NMR ($CDCl_2F$, 0 °C): δ 7.18 (m, 6H, 4-Me-C$_6$*H*$_4$), 7.07 (m, 6H, 4-Me-C$_6$*H*$_4$), 6.63 (s, 1H, CH), 6.03 (s, 1H, pz* H4/H4′), 5.92 (s, 1H, pz* H4/H4′), 3.09 (s, 1H, PdC*H*MeCH$_2$-μ-H), 2.36 (s, 9H, 4-*Me*-C$_6$H$_4$), 2.32 (s, 3H, pz* Me), 2.18 (s, 3H, pz* Me), 2.09 (s, 3H, pz* Me), 1.80 (s, 3H, pz* Me), −2.10 (br, ca. 5H,[29] PdCH*Me*C*H*$_2$-μ-*H*). ^{13}C NMR ($CDCl_2F$, 0 °C) δ 152.3 (3/3′-pz*), 142.7 (3/3′-pz*), 141.8 (5/5′-pz*), 141.5 (5/5′-pz*), 136.5, 129.9, 124.3, 107.9 (4/4′-pz*), 106.7 (4/4′-pz*), 63.5 (CH), 43.7 (Pd*C*HMeCH$_2$-μ-H), 20.7 (4-*Me*-C$_6$H$_4$), 14.1, 13.9, 11.0, 10.1; the PdCH*Me*CH$_2$-μ-H and PdCHMe*C*H$_2$-μ-H were not observed.

Generation of [{(*p*-tolyl)$_3$SiCH(pz*)$_2$}Pd(CH$_2$CH$_2$CH$_3$)(H$_2$C═CH$_2$)][B(C$_6$F$_5$)$_4$] by Reversible Ethylene Coordination (7). A valved NMR tube containing a CD_2Cl_2 (0.6 mL) solution of **6** (0.020 mmol) was cooled to −196 °C, and ethylene (0.020 mmol) was added by vacuum transfer. The sample was warmed to −60 °C for 1 h and placed in a precooled (−80 °C) NMR probe, and NMR spectra were recorded. The spectra showed that an equilibrium mixture of **6**, **7**, and free ethylene had formed. The equilibrium constant, $K_{eq} = [\mathbf{7}][\mathbf{6}]^{-1}[H_2C{=}CH_2]^{-1}$, was determined by ^{1}H NMR from −80 to −35 °C using the integrals of the (*p*-tolyl)Si*CH* resonances for **6** and **7** and the free ethylene resonance, referenced to the Et_2O internal standard. K_{eq} = 430 M^{-1} at −80 °C; $\Delta H = -7.4(5)$ kcal mol^{-1} and $\Delta S = -27(2)$ eu. The equilibrium expression was confirmed by two experiments in which [Pd] and [H$_2$C═CH$_2$] were varied. ^{1}H NMR (CD_2Cl_2, −80 °C): δ 7.26 (m, 6H, 4-Me-C$_6$*H*$_4$), 7.09 (m, 6H, 4-Me-C$_6$*H*$_4$), 6.70 (s, 1H, CH), 6.13 (s, 1H, pz* H4/H4′), 5.90 (s, 1H, pz* H4/H4′), 4.26 (br m, 4H, H$_2$C═CH$_2$), 2.39 (s, 12H, 4-*Me*-C$_6$H$_4$ and pz* Me), 2.04 (pz* Me), 1.94 (m, 2H, PdCH$_2$C*H*$_2$CH$_3$), 1.72 (s, 4H, pz* Me and PdC*H*$_2$CH$_2$CH$_3$), 0.77 (m, 4H, PdC*H*$_2$CH$_2$CH$_3$ and PdCH$_2$CH$_2$C*H*$_3$). ^{13}C{^{1}H} NMR (CD_2Cl_2, −80 °C): δ 150.5 (3/3′-pz*), 148.6 (3/3′-pz*), 142.2 (5/5′-pz*), 142.1, 140.9 (5/5′-pz*), 136.7, 129.5, 124.8, 108.3 (4/4′-pz*), 107.8 (4/4′-pz*), 64.0 (CH), 28.9 (PdCH$_2$*C*H$_2$CH$_3$), 23.7 (Pd*C*H$_2$CH$_2$CH$_3$), 21.6 (4-*Me*-C$_6$H$_4$), 15.1, 14.6, 12.7 (PdCH$_2$CH$_2$*C*H$_3$), 12.3, 11.2. Key ^{1}H – ^{1}H COSY interactions (CD_2Cl_2, −80 °C): δ 1.72 (PdC*H*$_2$CH$_2$CH$_3$) coupled to δ 0.77 (PdC*H*$_2$CH$_2$CH$_3$) and 1.94 (PdCH$_2$C*H*$_2$CH$_3$); δ 1.94 (PdCH$_2$C*H*$_2$CH$_3$) coupled to δ 0.77 (PdCH$_2$CH$_2$C*H*$_3$). A solution of **7** in $CDCl_2F$ was generated as described above, and variable-temperature (−80 to −115 °C) NMR experiments were conducted. ^{1}H NMR ($CDCl_2F$, −115 °C): δ 5.41 (br m, H$_2$C═CH$_2$), 4.54 (br m, H$_2$C═CH$_2$), 3.94 (br m, H$_2$C═CH$_2$), 2.83 (br m, H$_2$C═CH$_2$). ^{13}C{^{1}H} ($CDCl_2F$, −115 °C): δ 93.7 (br, H$_2$C═CH$_2$), 86.1 (br, H$_2$C═CH$_2$).[8] The rotational barrier $\Delta G_{rot}^{\ddagger} = 8.1$ kcal mol^{-1} was obtained from the coalescence of the δ 4.54 and 3.94 resonances, using the coalescence approximation (k_{rot} = 670 s^{-1} at $T_{coalescence}$ = −90 °C).[30]

(27) Daugulis, O.; Brookhart, M.; White, P. S. *Organometallics* **2002**, *21*, 5935.

(28) The oligomer mixtures were hydrogenated (MeOH, 1 atm of H_2, 10% Pd/C). GC-MS analysis of the product showed that a mixture of branched alkanes was formed.

(29) The integral is lower than expected due to peak broadness; $\Delta\nu_{1/2}$ = 250 Hz.

(30) The other two bound ethylene ^{1}H NMR resonances (δ 5.41, 2.83) were broadened into the baseline at −90 °C.

Generation of [{(*p*-tolyl)$_3$SiCH(pz*)$_2$}PdCHRCHR-μ-H][B(C$_6$F$_5$)$_4$] (8b, R = alkyl). A valved NMR tube containing a CH_2Cl_2 (0.6 mL) solution of **2** (13 mg, 0.020 mmol) and [Li(Et$_2$O)$_{2.8}$][B(C$_6$F$_5$)$_4$] (18 mg, 0.020 mmol) was cooled to −196 °C, and ethylene (1.1 mmol) was added by vacuum transfer. The solution was warmed to −10 °C for 6 h. The volatiles were removed under vacuum to yield a brown oily residue, which was washed with pentane (3 × 2 mL). The tube was evacuated and CD_2Cl_2 (0.6 mL) was added by vacuum transfer at −78 °C. The tube was transferred to a precooled (−80 °C) probe and spectra were recorded. The spectra established that **8** had formed in essentially quantitative yield. ^{1}H and ^{1}H–^{1}H COSY NMR experiments established that **8** comprises a mixture of species with a distribution of β-H agostic secondary alkyl complexes. The distribution of alkyl chains was established by methanolysis of the acyl complex **8a** described below. Key data for **8**: ^{1}H NMR (CD_2Cl_2; −80 °C): δ 7.16 (m, 6H, 4-Me-C$_6$*H*$_4$), 6.97 (m, 6H, 4-Me-C$_6$*H*$_4$), 6.37 (s, 1H, CH), 6.04 (s, 1H, pz* H4/H4′), 5.93 (s, 1H, pz* H4/H4′), 3.03 (m, 1H, PdC*H*RCHR-μ-H), 2.33 (s, 9H, 4-Me of 4-Me-C$_6$H$_4$), 2.29 (s, 3H, pz* Me), 2.13 (s, 3H, pz* Me), 2.06 (s, 3H, pz* Me), 1.69 (s, 3H, pz* Me), 0.42 (m, 1H, PdCHRC*H*R-μ-H), −9.50 (m, 1H, PdCHRCHR-μ-*H*). ^{1}H–^{1}H COSY correlations: Pd(CHC*H*(R)-μ-H)(R) to Pd(CHCH(R)-μ-*H*)(R) and Pd(CHC*H*(R)-μ-H)(R) to Pd(C*H*CH(R)-μ-H)(R). ^{13}C{^{1}H} NMR CD_2Cl_2; −80 °C): δ 151.9 (3/3′-pz*), 149.5 (3/3′-pz*), 142.8 (5/5′-pz*), 141.9, 141.1 (5/5′-pz*), 136.7, 129.2, 124.1, 108.0 (4/4′-pz*), 106.7 (4/4′-pz*), 63.5 (CH), 22.85 (4-*Me*-C$_6$H$_4$), 14.6 (pz* Me), 14.4 (pz* Me), 12.1 (pz* Me), 11.1 (pz* Me); the alky region is complex. The solution of **8** was warmed to 0 °C, and broadening of the PdCHRC*H*R-μ-*H* signals was observed. ^{1}H NMR (CD_2Cl_2, 0 °C): δ 7.15 (m, 6H, 4-Me-C$_6$*H*$_4$), 7.02 (m, 6H, 4-Me-C$_6$*H*$_4$), 6.47 (CH), 5.98 (s, 1H, pz* H4/H4′), 5.88 (s, 1H, pz* H4/H4′), 3.09 (br, 0.5H, *trans*-PdC*H*RCHR-μ-H, 2.72 (s, 0.5H *cis*-PdC*H*RCHR-μ-H), 2.32 (s, 9H, 4-*Me*-C$_6$H$_4$), 2.28 (s, 3H, pz* Me), 2.14 (s, 3H, pz* Me), 2.05 (s, 3H, pz* Me), 1.71 (s, 3H, pz* Me), −8.75 (br, 0.1H, PdCHRCHR-μ-*H*), −9.22 (br, 0.4H, PdCHRCHR-μ-*H*).[31]

Identification of the Distribution of Alkyl Chain Lengths in 8 by Carbonylation to Generate [{(*p*-tolyl)$_3$SiCH-(pz*)$_2$}Pd((C=O)(R)) CO][B(C$_6$F$_5$)$_4$] (8a) and Methanolysis to Give a Mixture of Esters. A valved NMR tube containing a CD_2Cl_2 (0.6 mL) solution of **8** (0.020 mmol) was cooled to −196 °C and exposed to CO (1 atm) for 5 min. The tube was sealed, warmed to −78 °C, and briefly warmed to 23 °C with vigorous shaking. A slurry of white solid in a colorless supernatant formed. The tube was kept at −78 °C and transferred to a precooled (−40 °C) NMR probe, and NMR spectra were recorded. The NMR spectra showed that **8a** had formed. Key NMR data: ^{1}H NMR (CD_2Cl_2, −40 °C; fast pz* exchange): δ 7.23 (m, 6H, 4-Me-C$_6$*H*$_4$), 7.17 (m, 6H, 4-Me-C$_6$*H*$_4$), 6.54 (s, 1H, C*H*), 6.03 (br s, 2H, pz* H4/H4′), 2.36 (s, 9H, 4-*Me*-C$_6$H$_4$), 2.16 (s, 6H, pz* Me), 1.76 (s, 6H, pz* Me); the alkyl region is complex. ^{13}C{^{1}H} NMR (CD_2Cl_2, −40 °C, for **8a** generated using ^{13}CO): δ 217.9 (*C*(O)R), 216.3 (*C*(O)R), 215.6 (*C*(O)Me), 215.5 (*C*(O)R), 215.3 (*C*(O)R), 215.3 (*C*(O)R), 212.4 (*C*(O)R), 212.2 (*C*(O)R), 172.9 (Pd*C*O), 172.8 (Pd*C*O), 172.7 (Pd*C*O), 171.8 (Pd*C*O), 142.4, 136.9, 129.5, 124.6, 63.4 (CH), 63.3 (CH), 21.5 (4-*Me*-C$_6$H$_4$); free CO was observed at δ 184.3; the pz* signals were broadened into the baseline due to pyrazole ring exchange; the alkyl region is complex. A solution of NaOMe in MeOH (0.050 mL, 0.4 M) was added to the solution of **8a**, resulting in the immediate formation of Pd^0. The mixture was exposed to air and diluted with hexanes (2 mL). The resulting black slurry was filtered through a pad of silica with hexanes/CH_2Cl_2 (10/1 by volume). The filtrate was analyzed by GC/MS, which showed that a mixture of C$_5$–C$_{17}$ alkyl methyl esters had formed.

Table 3. Summary of X-Ray Diffraction Data for 2·(3CHCl$_3$)

formula	C$_{64}$H$_{72}$Cl$_4$N$_8$Pd$_2$Si$_2$ + 6(CHCl$_3$)
fw	2080.29 (including solvent)
cryst size (mm)	0.25 × 0.25 × 0.25
D_{calc} (Mg/m^3)	1.543
cryst syst	triclinic
space group	$P\bar{1}$
a (Å)	13.379(2)
b (Å)	18.531(3)
c (Å)	20.735(4)
α (deg)	114.939(3)
β (deg)	103.056(3)
γ (deg)	92.893(3)
V (Å^3)	4478(1)
Z	2
temperature (K)	100
cryst color, habit	red-orange, fragment
goodness-of-fit on F^2	1.082
final R indices ($I > 2\sigma(I)$)[a]	R1 = 0.0479, wR2 = 0.1148
R indices (all data)[a]	R1 = 0.0538, wR2 = 0.1186

[a] R1 = $\sum F_o| - |F_c|/\sum|F_o|$; wR2 = $[\sum[w(F_o^2 - F_c^2)^2]/\sum[w(F_o^2)^2]]^{1/2}$, where $w = q[\sigma^2(F_o^2) + (aP)^2 + bP]^{-1}$.

Generation of [{((*p*-tolyl)$_3$Si)HC(pz*)$_2$}PdR(H$_2$C=CH$_2$)]-[B(C$_6$F$_5$)$_4$] (9). A valved NMR tube containing a solution of **8** (0.020 mmol) in CD_2Cl_2 (0.5 mL) containing Et$_2$O (0.060 mmol, as an internal standard) was cooled to −196 °C, and ethylene (0.82 mmol) was added by vacuum transfer. The tube was thawed at −78 °C and transferred to a precooled (−80 °C) NMR probe. NMR spectra showed that an equilibrium mixture of **8**, **9**, and free ethylene had formed. The equilibrium constant, $K_{eq} = [\mathbf{9}][\mathbf{8}]^{-1}[H_2C{=}CH_2]^{-1}$, was determined by ^{1}H NMR from −80 to −55 °C using the integrals of the (*p*-tolyl)$_3$SiC*H* resonances for **8** and **9** and the free ethylene resonance, referenced to the Et$_2$O internal standard. $K_{eq} = 35$ M^{-1} at −80 °C. The resonances for the alkyl group (distribution of chain lengths) could not be assigned because they overlap with those of the N^N ligand and **8**. Key data for **9**: ^{1}H NMR (CD_2Cl_2, −80 °C): δ 7.20 (m, 6H, 4-Me-C$_6$*H*$_4$), 7.02 (m, 6H, 4-Me-C$_6$*H*$_4$), 6.69 (CH), 6.08 (s, 1H, pz* H4/H4′), 5.82 (s, 1H, pz* H4/H4′), 4.15 (br m, 4H, Pd(H$_2$C=CH$_2$)), 2.33 (s, 9H, 4-*Me*-C$_6$H$_4$), 2.28 (s, 3H, pz* Me), 1.97 (br s, 3H, pz* Me), 1.63 (s, 3H, pz* Me); the alky region is complex. ^{13}C{^{1}H} NMR ($CDCl_2F$, −100 °C): δ 151.2 (3/3′-pz*), 150.3 (3/3′-pz*), 142.6, 142.0 (5/5′-pz*), 140.9 (5/5′-pz*), 136.9, 129.4, 124.8. 108.5 (4/4′-pz*), 108.3 (4/4′-pz*), 93.1 (br, Pd(H$_2$C=CH$_2$)), 85.3 (br, Pd(H$_2$C=CH$_2$), 63.8 (CH), 21.2 (4-*Me*-C$_6$H$_4$), 14.6 (pz* Me), 12.2 (pz* Me), 11.8 (pz* Me), 10.7 (pz* Me); the alkyl region is complex. A solution of **9** in $CDCl_2F$ was generated as described above, and variable-temperature (−80 to −120 °C) NMR spectra were measured. ^{1}H NMR ($CDCl_2F$, −120 °C): δ 4.45 (br m, 1H, Pd(H$_2$C=CH$_2$)), 3.91 (br m, 1H, Pd(H$_2$C=CH$_2$)), 3.57 (br m, 1H, Pd(H$_2$C=CH$_2$)), 2.75 (br m, 1H, Pd(H$_2$C=CH$_2$)). The rotational barrier $\Delta G^{\ddagger} = 8.3$ kcal mol^{-1} was obtained from the

(31) The integrals for the agostic-H signals are low due to exchange between agostic and nonagostic β-hydrogens. For dynamics of cationic β-H-agostic Pd alkyl complexes see: Shultz, L. H.; Tempel, D. J.; Brookhart, M. *J. Am. Chem. Soc.* **2001**, *123*, 11539.

coalescence of the δ 3.91 and 3.57 resonances, using the coalescence approximation ($k_{rot} = 380\ s^{-1}$ at $T_{coalescence} = -90$ °C).[32]

Measurement of pz* Exchange Rates. pz* exchange rates for **3**, **4**, **7**, and **9** were determined by variable-temperature ^{1}H NMR spectroscopy. Rate constants (k_{exch}) were determined by simulation of the pz* H4/H4′ line shapes using gNMR.[33] The line width of the (*p*-tolyl)$_3$SiC*H* resonance was used as the line width in the absence of exchange. The measured k_{exch} values were independent of [Pd], and of the [free CO] for **4** and [free ethylene] for **7**. Activation parameters were determined from Eyring plots for each run.

X-Ray Crystallographic Analysis of {(*p*-tolyl)$_3$SiCH(3,5-Me$_2$-pz)$_2$}PdCl$_2$ (2). Single crystals of **2** were obtained by slow diffusion of pentane into a concentrated $CHCl_3$ solution at 23 °C. Crystallographic data are summarized in Table 3. Data were collected on a Bruker Smart Apex diffractometer using Mo Kα radiation (0.71073 Å). The space group was determined as $P\bar{1}$ based on systematic absences and intensity statistics. Direct methods were used to locate the Pd, Cl, Si, and most C atoms from the E-map. Repeated difference Fourier maps allowed recognition of all expect C and N atoms. Following anisotropic refinement of all non-H atoms, ideal H atom positions were calculated. Final refinement was anisotropic for non-H atoms and isotropic-riding for H atoms. The asymmetric unit contains two molecules of **2**, which differ only in the orientation of the apical Si(*p*-tolyl)$_3$ group due to rotation around the (*p*-tolyl)$_3$Si−CH(3,5-Me$_2$-pz)$_2$ bond, and six $CHCl_3$.

(32) The other two ethylene ^{1}H NMR resonances (δ 4.45, 2.75) were broadened into the baseline at −90 °C.

(33) *gNMR, v. 4.1.2b*; Adept Scientific: Letchworth, UK, 2000.

Acknowledgment. This work was supported by the U.S. Department of Energy (DE-FG-02-00ER15036).

Supporting Information Available: NMR data, synthetic procedures, determination of ethylene binding constants and pz* site exchange rates, and complete mechanism of pz* exchange. This material is available free of charge via the Internet at http://pubs.acs.org.

OM7007698